Intestinal Barrier Disruption as a Cause of Mortality in Combined Radiation and Burn Injury

Stewart R Carter[1,2], **Anita Zahs**[1,2], **Jessica L Palmer**[1,2], **Lu Wang**[4], **Luis Ramirez**[1,2], **Richard L Gamelli**[1,2], and **Elizabeth J Kovacs**[1,2,3]

[1]Burn and Shock Trauma Research Institute, Loyola University Chicago Health Sciences Division, Maywood, IL 60153

[2]Department of Surgery, Loyola University Chicago Health Sciences Division, Maywood, IL 60153

[3]Department of Microbiology & Immunology, Loyola University Chicago Health Sciences Division, Maywood, IL 60153

[4]Department of Pathology, Loyola University Chicago Health Sciences Division, Maywood, IL 60153

Introduction

Combined radiation injury (CRI) occurs following nuclear disaster, such as reactor accidents or nuclear detonations. Injuries in addition to radiation exposure include trauma, burns, chemical exposures and infectious complications. Casualty estimates based on previous atomic bomb detonations predict that 65-70% of victims of CRI will have traumatic injury in addition to radiation exposure, while only 15-20% will be affected by radiation alone (1). This has been illustrated by the tragedies of the second world war that took place in Hiroshima and Nagasaki, Japan, resulting in greater than 60% of radiation victims also having sustained traumatic injuries (1, 2).

CRI results in higher mortality and worse complications than isolated radiation exposure or trauma, with victims sustaining injuries to nearly every organ system (3, 4) and cardiovascular, neurologic, hematopoetic and gastrointestinal (GI) effects are the most severe (5). Intestinal involvement following CRI is a contributor to early death (6). Therefore, hypotheses accounting for higher morbidity and mortality associated with CRI should focus on the intestine's function as a barrier to endotoxins and intraluminal bacteria that inhabit the gut.

Both isolated radiation injury and cutaneous burn indirectly results in the breakdown of the GI barrier by remarkably similar mechanisms. Ionizing radiation alters the organization of integral components of tight junctions, such as occludin, ZO-1 and -catenin, resulting in increased gut permeability (7-9). Radiation exposure generates reactive oxygen species (ROS) causing single and double stranded DNA breaks and intracellular alterations resulting in apoptosis, autophagy and subsequent breakdown of the gut epithelium (10). Increased cell

Corresponding Author: Elizabeth J. Kovacs, PhD, Loyola University Medical Center, 2160 South First Avenue, Maywood, IL 60153, 708-327-2477, ekovacs@lumc.edu.

Conflicts of Interest: The authors of this manuscript have no conflicts of interest to report.

death, specifically affecting mitotically active cells, delays epithelial repair, allowing penetration of antigens, bacterial products and digestive enzymes. An intense inflammatory response ensues (10, 11).

Cutaneous burn indirectly decreases levels of tight junction proteins in the intestinal epithelium, resulting in a burn-induced gut barrier injury (12). Further disruption is mediated through increased apoptosis of epithelial cells as well as dysfunctional proliferation (13). Production of gut-derived pro-inflammatory mediators, which travel through the intestinal lymphatics, have been implicated in a systemic inflammatory response and shock observed after isolated burn (14, 15).

To our knowledge, GI involvement in CRI has not been reexamined since early descriptive studies following the second world war (6). Disruption of cell proliferation, increased apoptosis and the effects of burn and radiation on tight junctions could diminish intestinal barrier function and make victims susceptible to bacterial translocation and subsequent death due to septic shock. Even in the setting of a smaller burn wound, or sub lethal dose of radiation exposure, the combination of these disturbances can trigger or elevate gut leakiness resulting in increased morbidity and mortality. The purpose of this study is to determine if the combined effects of radiation and burn cause GI permeability as a possible explanation for increased mortality not present with isolated injury types.

Materials and Methods

Animals

Eight to ten week-old male (C57BL/6, 23-25g) mice were obtained from Charles River Laboratories (Wilmington, MA), and housed in sterile microisolator cages at the Loyola University Medical Center Comparative Medicine Facility. All animal studies described here were approved and performed with accordance to the guidelines established by the Loyola University Institutional Animal Care and Use Committee.

Combined irradiation and burn injury

A model previously described by our group was utilized to administer isolated burn, isolated radiation and combined injuries (16) with minor modifications. The radiation dose was adjusted between 5.0-5.5 Gy total body irradiation (TBI) in order to maintain a mortality rate among CRI animals between 40-60%. Approximately one hour following radiation injury, mice were anesthetized with a mixture of ketamine (100 mg/kg) and xylazine (10 mg/kg) i.p., their dorsal surfaces were then shaved. Mice were placed into a plastic template exposing 15% total body surface area (TBSA), as calculated by previously described methods (17, 18). Scald injury was performed in 90-92°C water bath or sham injury in room temperature water. Animals were dried immediately following burn to prevent further scalding. All animals received 1.0 ml of warmed 0.9% normal saline i.p. resuscitation immediately after the burn injury and cages were placed on heating pads while the animals recovered from anesthesia. At 24, 48 and 72 hr after injury, mice were euthanized by CO_2 narcosis followed by exsanguination. Animals that expired prior to designated study time points were included only in survival data and tissues were not processed for further studies. The sequence of radiation injury then burn was necessary due to location of the radiation source at another facility and difficulties associated with transporting mice recovering from burn injury.

Bacterial Translocation

Bacterial translocation was assessed as previously described with minor modifications (19, 20). At 24 and 72 hr following injury, using sterile technique, for each mouse the mesenteric

lymph node (MLN) complex was removed and placed in cold RPMI with 5% fetal bovine serum on ice. Nodes were dissected out from surrounding mesenteric fat taking note of the total number of lymph nodes isolated, transferred and homogenized in 500μl of RPMI. Aliquots of 100μl were then plated in triplicate (300μl total) on tryptic soy agar plates and placed in a 37°C incubator overnight providing a lower limit of detection of <2 CFU. Colonies were counted the following day. For each animal, the total number of colony forming units (CFU) from the three plates was determined and divided by the total lymph nodes harvested from the MLN complex. Values obtained for each animal were grouped according to injury and final averages were determined for comparison. In the event that no colonies were recovered, an estimated value of <2 CFU/ml was assigned.

Histopathology and Apoptosis Scoring

Distal ileum, was harvested at 24, 48 and 72 hr time-points following injury. Tissue was suspended in 10% formalin, sectioned and stained with hematoxylin and eosin (H&E). A pathologist, who was blinded to the experimental groups, evaluated specimens for the presence of apoptotic bodies using a scoring system we developed. All quantification was performed at 40× magnification. The presence of apoptotic bodies was scored 0-4, 0 being none, 1 being one per four intestinal crypts, 2 being two per four crypts, 3 being three per four crypts, and 4 being four or more apoptotic bodies per four crypts.

Cell Death Detection

Total apoptosis was quantified using the Cell Death Detection ELISA[PLUS] (Roche-Applied-Science) as previously described (13). Whole ileum was homogenized utilizing Bio-Plex Lysis Buffer (Bio Rad). Protein concentration of lysate was determined by total protein assay. Reported data are expressed as optical density per 15 μg protein.

Western Blot Analysis

Western blot was performed as previously described (20) with minor modifications. Thirty micrograms of whole cell lysate protein was boiled for 5 minutes, separated by sodium dodecyl sulfate polyacrylamide gel electrophoresis, transferred to polyvinylidene fluoride membranes and blotted with primary antibodies specific for anti-caspase-3 (Abcam, Cambridge, MA), anti-caspase-8 (Abcam), and -tubulin (Abcam). For antibodies that recognized multiple forms of the protein at different molecular weights (caspase-3 and caspase-8), all bands were quantified from the same sample relative to the loading control from that lane using BioRad Image Lab software. Normalized values obtained from densitometry were then expressed as fold change relative to sham. Alternatively, membranes were blotted with rabbit anti-occludin (Life Technologies Corporation, Carlsbad, CA), and -actin (Cell Signaling Technology, Danvers, MA). Quantification of occludin was performed similarly to that of caspase levels, with normalization to -actin, and presentation of data as fold change relative to sham.

Immunofluorescent Staining of Occludin

Ileum was sectioned and embedded in OCT at time of euthanasia and frozen for immunofluorescent staining as previously described (20) with minor modifications. Sections were cut 8 μm thick and stained with rabbit anti-occludin antibody (Life Technologies) followed by goat anti-rabbit AlexaFluor 488 antibody (Life Technologies). Sections were counterstained with fluorescent-conjugated phalloidin (actin) and Hoechst nuclear stain (Life Technologies). Using Zeiss software (model LSM 510, version 4.2 SP1), a 20-epithelial cell section (crypt or villus) was outlined. Within this section, the number of co-localized red and green pixels was determined. This number was then divided by the total number of pixels within the section and expressed as a percentage. This process was

repeated on 4 sections per animal, leading to a total of 100 epithelial cells examined for each animal. Averaged results per animal were used to determine treatment group averages.

Statistical Analysis

Statistical analyses (GraphPad Prism) were performed comparing 4 total groups including sham, burn, radiation (RAD), and CRI (RAD+BURN). Differences in survival between groups was analyzed using Kaplan-Meier Survival Analysis with a log-rank significance test. For apoptosis scoring, differences in non-parametric data were noted among injury groups and analysis was conducted using one-way analysis of variance followed by a Dunn's Multiple Comparison post-hoc test if significance was achieved ($p<0.05$). For bacterial translocation, western blot densitometry, histone-associated DNA fragment ELISA and quantification of percent co-localization between occludin and actin filaments, one-way analysis of variance was performed followed with Tukey-Kramer Multiple Comparisons post-hoc test if significance was achieved ($p<0.05$).

Results

Increased mortality at 72 hr following CRI

Based on previous studies utilizing a murine model of CRI established in our laboratory (16), we have consistently observed a 40 – 60% mortality rate associated with 15% TBSA scald combined with 5-6 Gy TBI by the third day post-injury. A 15% TBSA scald burn alone has been extensively studied and it is rare that it alone causes mortality in young mice (18, 21). We have also shown that radiation alone does not cause mortality until dosing approaches 11 Gy TBI in mice (16). These findings were comparable with the current experiment (Figure 1). CRI demonstrated an expected increase in animal death by 72 hr, with only 58.8% surviving ($p<0.05$). No deaths occurred in sham animals at any time point. A single mouse exposed to burn alone died prior to the 24 hr time point. There was a 12.5% mortality rate in this group at 72 hr, demonstrating the rare, but possible occurrence of death in this group. Only a single radiation alone animal died prior to 24 hr, otherwise there were no casualties.

Evidence of bacterial translocation 72 hr following CRI

Mesenteric lymph nodes were harvested following euthanasia at 24 and 72 hr post injury, homogenized, and plated on tryptic soy agar. Bacterial growth was observed in burn alone animals at 24 hr post injury with approximately 5.0×10^1 CFU/MLN ($p<0.05$ vs. all groups). At 72 hr post injury, only CRI exhibited significant bacterial growth with approximately 1×10^2 CFU/MLN ($p<0.05$ vs. all groups) (Figure 2).

Alterations in quantity and distribution of occludin after CRI correlates with evidence of epithelial barrier dysfunction at 72 hr

With the observation of increased bacterial translocation at 72 hr, we wanted to determine if alteration in distribution of gastrointestinal tight junctions preceded gut permeability by staining and quantifying occludin protein co-localization with actin. Immunofluorescence (IF) showed less evident staining of occludin along the apical border of the epithelium and diminished co-localization in radiation alone and CRI animals (Figure 3). Sham animals averaged 10-11% co-localization of occludin and actin at all time points. Burn animals had slightly diminished co-localization at 24 and 48 hr time points at 9% and 8% respectively, which returned to sham levels by 72 hr. None of these differences reached statistical significance. Radiation alone animals had approximately half the amount of co-localization of sham at 24 and 48 hr ($p <0.05$ vs. sham and burn), but returned to 80% at 72 hr. CRI had the largest decreases in co-localization at all time points with 3% and 2%, respectively at 24

and 48 hr (p <0.05 vs. sham and burn) and 4% at 72 hr (p <0.05 vs. all groups) (Figure 4). Levels following CRI were 50% lower than radiation alone at all time points. In order to determine if changes were due to alterations in occludin organization or decreased total protein due to injury, we performed quantification by western blot analysis. Occludin (65 kDa) measurement by densitometry was decreased relative to sham at 42% and 33% at 24 hr in radiation alone and CRI respectively (p<0.05). This trend persisted at 48 hr with levels that were 46% and 27% of sham (p<0.05). At 72 hr post-injury, radiation alone was no longer significantly different from sham, whereas CRI remained lower relative to both sham and burn alone (24%, p<0.05) (Figure 5).

Evidence of prolonged apoptosis 48 hr following CRI

In order to determine if greater damage to intestinal lining correlated with tight junction disruption, we sought to characterize and quantify epithelial cell apoptosis following injury. High power images stained with H&E were used for quantification of apoptosis in distal ileum sections. We developed a scoring system in order to compare treatment groups. Apoptotic cells were more numerous in animals that underwent radiation. Sham animals had median scores of 0 for apoptotic cells present at all time points. Burn alone animals had median scores of 2, 1 and 0 at 24, 48 and 72 hr respectively, none of which achieved statistical significance. Radiation alone animals had a median score of 1 and 2 at 24 hr and 48 hr respectively (p<0.05 vs. sham). Apoptosis remained elevated at 72 hr with a median score of 2, which was significantly higher than sham and burn alone at the same time point (p<0.05). Quantification of apoptotic cells in CRI was persistently elevated, with values of 3, 4 and 3 at 24, 48 and 72 hr respectively (p<0.05 vs. sham at all time points, p<0.05 vs. burn at 48 and 72 hr) (Figure 6).

Following observations of a prolonged increase in epithelial apoptosis in the ileum of CRI-exposed mice, we performed a quantitative analysis of whole ileum cell death. Histone-associated DNA fragments were measured as an indirect assessment of apoptosis in injury groups at 24, 48 and 72 hr after initial injury. Twenty-four hours post injury, radiation injury alone exhibited a 2 fold increase in histone associated DNA fragments relative to sham (p<0.05). At 48 hr, there was a 3-fold increase in apoptosis in the CRI group relative to all other injury groups (p<0.05). Radiation injury alone was comparable to sham and burn alone at this time point. Levels of apoptosis approached sham level values in all injury groups at 72 hr post-injury (Figure 7).

To further characterize apoptosis, caspases-3 and caspase-8 (pro and cleaved forms) protein levels were examined in injury groups at 24, 48 and 72 hr time points. Pro-caspase-3 trended towards elevation in burn alone at 24 and 48 hr post injury (2 fold increases at both time points), in CRI at 48 and 72 hr (4 and 3 fold increases respectively), and in radiation injury alone at 72 hr (3 fold increase). Similarly levels of caspase-3 trended towards elevation in CRI at 48 and 72 hr (both over 2-fold), but did not reach significance elevated at any time point in any injury group (Figure 8).

The pro-form of caspase-8 was elevated approximately 13 fold at 48 hr, and 5 fold at 72 hr relative to sham expression. Burn alone animals also had increases in pro-caspase-8 by 4 fold at 48 hr and 3 fold at 72 hr, although these values were not statistically different. Significant elevation of caspase-8 occurred at 24 hr post-injury in burn alone animals with a 2 fold higher levels relative to sham at the same time point (p<0.05). Levels in CRI animals at 48 hr were found to be approximately 3 times that of time matched sham and radiation alone animals (p<0.05) (Figure 9).

Discussion

While the potential for nuclear disaster seems remote, it presents an intimidating problem, specifically in the medical management of survivors. Combined radiation injury commonly affects victims in such events, and while knowledge of the nature of these injuries has been present since the Second World War (3, 4) little is known about the mechanism by which CRI increases morbidity and mortality. Despite concerted research efforts, clear treatment options to improve acute survival remain largely undetermined in humans outside of supportive care (22, 23). Given the systemic nature of total body irradiation, as well as large cutaneous burns, damage to individual organ systems will contribute to a more severe wide spread condition. Our murine model of CRI provides a way of better understanding effects of such a rarely occurring, yet devastating problem in order to elucidate possible pathways contributing to increased death (16). To our knowledge, we are the first to present GI findings of this nature in any CRI model with the exception of early studies on CRI in the 1960s (6). Increased knowledge of mechanisms behind elevated mortality in CRI can guide resuscitative efforts, develop therapies for organ specific damage, and attenuate the resulting systemic inflammatory response. The gastrointestinal tract is known to be particularly radiosensitive and is an excellent initial target for proposed therapeutics in CRI (5).

Early mortality following a nuclear disaster is often attributed to gastrointestinal involvement with death secondary to infection, septic shock, dehydration, and severe electrolyte imbalances (6, 22). Our observations of early time points in mouse ileum exposed to CRI confirm the destructive nature of this injury and suggest that a combination of apoptotic activity with suppression of normal cell proliferation are present, much like in isolated burn or radiation exposures. Previous work with isolated burn injury shows organ specific elevation of caspase-3 following 20% TBSA burn within the first few hours of injury for spleen and thymus (24) and 6-12 hours after 30% TBSA burn by TUNEL stain and histone-associated DNA fragmentation in the intestine (13, 25). Similarly, ionizing radiation is responsible for ROS resulting in single and double stranded DNA breaks triggering apoptosis. Both isolated burn and radiation injuries are also with linked to aberrant epithelial cell proliferation (10-13). Given the nature of these injuries, we wanted to determine if the combination would result in evidence of loss of gut barrier integrity not present following isolated injuries.

Bacterial translocation was present with the combined insult, although at a later time point than other studies (15, 19). A modest increase in bacterial translocation was seen in burn alone animals at 24 hr. While statistically significant, it is low at 5×10^1 and likely would not result in systemic responses large enough to result in animal death. Seventy-two hours post-injury, CRI animals exhibited a significant increase in bacterial accumulation in MLN, which may be due to the prolonged intestinal damage seen in these animals in conjunction with immunosuppression consistent with radiation exposure (Figure 1). No other injury group had bacteria in MLN at 72 hr post injury. Given the multiple insults occurring in victims of CRI, it is plausible that opportunistic bacteria could overwhelm the host, leading to septic shock and death.

In order to examine possible causes for the elevated bacterial translocation seen in the CRI group, we investigated the effects of combined injury on GI epithelial tight junctions relative to isolated burn and radiation injuries. We found that radiation exposure disorganizes tight junctions, as evidenced by decreased relative amounts and altered distribution of occludin protein. These findings are consistent with effects on occludin seen with ionizing radiation as well as decreased amounts of the protein in isolated burn injury (7-9, 15). Changes in gut barrier integrity would explain bacterial translocation seen 72 hr after animals were exposed to CRI. Occludin is an important transmembrane protein involved in the maintenance tight

junctions. Assembly and disassembly of tight junctions is determined by phosphorylation on either serine and threonine, or tyrosine residues of this protein (26). Measurement of the 65kDa protein is not suggestive of states of tight junction assembly, but does reflect differences following exposure to CRI. The 65 kDa form of occludin was significantly lower in radiation alone and CRI based on western blot analysis (Figure 5). Decreases in densitometry were lowest in the combined injury group at all time points indicating that protein levels were still affected three days after initial injury. Alterations in percent co-localization and western blot findings trended similarly (Figure 4, 5). Diminished staining for occludin seen by IF in radiation treated animals suggests decreased overall levels (Figure 3), however immunoprecipitation of phosphorylated forms may be necessary to assess total quantity of occludin or its role in tight junction maintenance following CRI.

Some discrepancy of image size in Figure 3 is noted at 48 hr, specifically in the burn injury (f) and combined injury groups (h). Images were selected to be representative of occludin colocalization for an injury group and similar in villus size and shape within a specific time point. Villi appear to be wider despite being taken with the same objective (40×). A slight increase in overall magnification was noted when comparing 48 hr to the 24 and 72 hr time points, which is evident when looking at the 20 μm scale. Another factor which could affect villus size following burn is the development of interstitial edema due to increased endothelial permeability (27). This may account for the broader villi seen in the burn alone and combined injury treated groups, specifically at the 48 hr time point. Despite the discrepancy in magnification, this had no effect on calculation of % colocalization of pixels per 100 epithelial cells or on occludin content by Western Blot analysis.

Increased apoptosis may contribute to alterations in intestinal epithelial barrier function including tight junction assembly and maintenance. CRI differs from isolated burn or radiation with histology showing continued apoptosis 72 hr after it has subsided in isolated injury groups. Prolongation of apoptosis is occurring simultaneously with increased crypt debris, either from tissue destruction, disrupted clearance or both, and a delay in recovery of mitosis (data not shown). In contrast, animals given burn or radiation alone have either recovered or are recovering prior to 48 hr post injury. Further support for prolonged apoptosis at 48 hr post-injury in CRI is seen by histone associated DNA fragmentation (Figure 7). This measurement was made using whole ileum homogenate as opposed to isolated epithelial cells, which may explain inconsistencies seen with histologic scoring in other injury groups, specifically radiation injury alone at 48 and 72 hr. Apoptosis occurring in intestinal tissue other than the epithelium, such as endothelium, may account for these differences. Evidence of apoptotic enzyme activity peaking at 24 to 48 hr is seen with western blot analysis of the extrinsic pathway of apoptosis (Figures 8, 9). While caspase-3 was not observed to be elevated, it's upstream component in the activation cascade, caspase-8, was elevated at 48 hr, suggesting that caspase-3 activation might follow at a later time point (between 48 and 72 hr). Caspase-3 is rapidly degraded in vivo; therefore tissue processing for western blot analysis may contribute to the lack of significant elevation seen in our analysis. Techniques for stabilization of caspase-3 utilizing caspase inhibitors have been described (28). Despite a lack of significant elevation, trends in CRI point towards increased intestinal capase-3 activity. Histology, histone-associated DNA fragmentation ELISA and caspase quantification by western all suggest enhanced apoptotic activity in CRI 48 hr after initial injury and beyond when compared to either burn or radiation alone.

Elevated levels of pro-caspase-8 occurring at 48 and 72 hr suggest another explanation for discrepancies in caspase-3 activity and increased mortality. In some cell types, inhibition of caspase-8 has been shown to activate pathways mediated by tumor necrosis factor (TNF) resulting in necrotic cell death (29). Inactivation of caspases has been implicated in a shift from apoptosis either to cell death morphologies with mixed necrotic and apoptotic features

or necrosis termed necroptosis (30). Necroptosis is dependent on the serine/threonine kinase activity of receptor-interacting protein kinase 1 and 3 (RIPK-1 and RIPK-3) (30). Active caspase-8 has been implicated in cleaving and inactivating proteins RIPK-1 and RIPK-3, two components of a complex termed the ripoptosome, which must be enzymatically active for the execution of necroptosis (31). Elevation of pro-caspase-8 in CRI at 48 and 72 hr may indicate a shift from apoptotic activity to necroptosis, or concurrent activity. Further elucidation of the role of necroptosis in CRI could explain gut-induced morbidity without significant elevation of caspase-3.

Findings of tight junction alterations and prolonged cell death in CRI correlate with the observed increase in bacterial translocation and mortality of greater than 40% at 72 hours post injury. Mice that did not survive to assigned time points were not included in this study; therefore, it is possible that the findings of this study would be more severe in these animals. Despite the correlation between bacterial translocation and gastrointestinal morbidity, this may not solely account for increases in mortality. It is likely that other organ systems damaged by CRI, such as cardiovascular, neurologic, hematopoeitic and pulmonary systems are involved in animal death. However, the GI tract remains a major source of early mortality. Therapies directed at attenuating sequelae of CRI such as bacterial translocation would be expected to improve acute survival following injury. From these data it is not clear whether the combined effects of radiation and burn are additive or if modest burn amplifies the effects of sub-lethal radiation.

One might suggest a two hit phenomenon is occurring in ileum of animals exposed to CRI. The initial insult occurs at the time of injury and consists of ROS and inflammatory responses with elevations in serum IL-6, and TNF , which have been shown at 6 and 48 hr time points in CRI using this model (16). Another study corroborates inflammation occurring well after the initial injury utilizing a similar murine model. Three days following exposure to 5 Gy TBI combined with a 20% TBSA burn with a heated rod, serum pro-inflammatory cytokines were elevated, specifically IL-5, IL-6, IL-10, IL-12 and MCP-1 (32).Disorganization of tight junctions and a prolonged state of apoptosis at 24 to 48 hr post-exposure contributes to epithelial breakdown, allowing penetration of endotoxins, bacteria and other harmful substances well beyond the initial exposure. This could potentially explain increases in acute mortality following CRI when isolated radiation and burn injury fail to produce similar results. This second hit provides a window in which therapeutics could be administered in order to attenuate intestinal epithelial damage and assist regeneration of the gut epithelium. Blocking the apoptotic response seems like less of a viable option. Inhibiting caspase-8 mediated apoptosis in some cell lines has induced TNF mediated necrosis (33). However, attenuating gut leakiness could prevent bacterial translocation and the subsequent inflammatory response. Myosin light chain kinase is an important enzyme in the maintenance of the mucosal barrier of the intestine. Under inflammatory conditions, it has been shown to alter myosin-actin interactions by phosphorylation of the myosin light chain, resulting in cytoskeletal sliding and tight junction disruption (34). Cell-permeating peptide inhibitors of myosin light chain kinase, such as permeant inhibitor of MLCK (PIK), have been found to reduce occludin disorganization away from tight junctions following inflammatory states such as in a model of combined ethanol and burn injury. PIK could be used as an investigational agent in our model of CRI as well (35).

The use of nuclear technology, and the potential for its implementation in warfare and terrorism highlight the importance of this study. Animal models will be paramount in the development of therapeutics in preparation for such events. Insight into the effects of CRI on the gut will help direct management of survivors of nuclear disaster. Further research into

the mechanistic targets underlying gut related morbidity and mortality associated with CRI may enable development of effective mitigating agents.

Acknowledgments

References

1. Pellmar TCLGD. Combined Injury - Radiation in Combination with Trauma, Infectious Disease, or Chemical Exposures. NATO RTG-099. 2005; 19:1–9.

2. Johnson AM. Pulmonary effects of combine the blast injury and radiation poisoning. J R Army Med Corps. 2004; 150:22–26. [PubMed: 15615107]

3. Brooks JW, Evans EI, Ham WT Jr. Reid JD. The influence of external body radiation on mortality from thermal burns. Ann Surg. 1952; 136:533–545. [PubMed: 14953182]

4. Alpen EL, Sheline GE. The Combined Effects of Thermal Burns and Whole Body X-Irradiation on Survival Time and Mortality. Ann Surg. 1954; 140(1):113–118. [PubMed: 13159151]

5. DiCarlo AM C, Hick J, Hanfling D, Daniak N, Chao N, Bader J. Radiation Injury After a Nuclear Detonation: Medical Consequences and the Need for Scarce Resources Allocation. Disaster Med Public Health Prep. 2011; 5(Suppl 1):S32–44. [PubMed: 21402810]

6. Baker DG, Valeriote FA. The effect of x-irradiation and thermal burn on the intestinal mucosa. Can J Physiol Pharmacol. 1968; 46(3):533–536. [PubMed: 5698923]

7. Somosy Z, Horvath G, Telbisz A, Rez G, Palfia Z. Morphological aspects of ionizing radiation response of small intestine. Micron. 2002; 33(2):167–178. [PubMed: 11567886]

8. Somosy Z, Bognar G, Thuroczy G, Koteles GJ. Biological responses of tight junction to ionizing radiation and electromagnetic field expostion. Cell Mol Biol. 2002; 48(5):571–575. [PubMed: 12146714]

9. Dublineau I, Lebrun F, Grison S, Griffiths NM. Functional and structural alterations of epithelial barrier properties of rat ileum following X-irradiation. Can J Physiol Pharmacol. 2004; 82(2):84–93. [PubMed: 15052289]

10. Hauer-Jensen, M.; Kumar, KS.; Wang, J.; Berbee, M.; Fu, Q.; Boerma, M. Larche RA: *Global Terrorism Issues and Developments 2007*. Nova Science Publishers; 2007. Intestinal Toxicity in Radiation - and Combined Injury: Significance, Mechanisms, and Countermeasures. Chapter 2:1-38

11. Kiang JG, Garrison BR, Gorbunov NV. Radiation Combined Injury: DNA Damage, Apoptosis, and Autophagy. Adapt Med. 2010; 2(1):1–10.

12. Costantini TW, Loomis WH, Putnam JG, Drusinsky D, Deree J, Choi S, et al. Burn-induced gut barrier injury is attenuated by phosphodiesterase inhibition: effects on tight junction structural proteins. SHOCK. 2009; 31(4):416–422. [PubMed: 18791495]

13. Wolf SEI H, Matin S, Debroy MA, Rajaraman S, Herndon DN, Thompson JC. Cutaneous Burn Increases Apoptosis in the Gut Epithelium of Mice. J Am Coll Surg. 1999; 188(1):10–16. [PubMed: 9915236]

14. Magnotti LJU JS, Xu D-Z, Lu Q, Deitch EA. Gut-Derived Mesenteric Lymph but not Portal Blood Increases Endothelial Cell Permeability and Promotes Lung Injury After Hemorrhagic Shock. Ann Surg. 1998; 228(4):518–527. [PubMed: 9790341]

15. Choudhry MA, Chaudry IH. Alcohol, burn injury, and the intestine. J Emerg Trauma Shock. 2008; 1:81–87. [PubMed: 19561986]

16. Palmer JL, Deburghgraeve CR, Bird MD, Hauer-Jensen M, Kovacs EJ. Development of a combined radiation and burn injury model. J Burn Care Res. 2011; 32(2):317–323. [PubMed: 21233728]

17. Spector WG, Willoughby DA. Experimental suppression of increased capillary permeability in thermal burns in rats. Nature. 1958; 182(4640):949–950. [PubMed: 13590187]

18. Faunce DE, Gregory MS, Kovacs EJ. Effects of acute ethanol exposure on cellular immune responses in a murine model of thermal injury. J Leukoc Biol. 1997; 62(6):733–740. [PubMed: 9400814]

19. Kavanaugh MJ, Clark C, Goto M, Kovacs EJ, Gamelli RL, Sayeed MM, et al. Effect of acute alcohol ingestion prior to burn injury on intestinal bacterial growth and barrier function. Burns. 2005; 31(3):290–296. [PubMed: 15774282]

20. Zahs A, Bird MD, Ramirez L, Choudhry MA, Kovacs EJ. Anti-IL-6 Antibody Treatment but Not IL-6 Knockout Improves Intestinal Barrier Function and Reduces Inflammation After Binge Ethanol Exposure and Burn Injury. SHOCK. 2013; 39(4):373–379. [PubMed: 23376955]

21. Walker HL, Mason AD Jr. A standard animal burn. J Trauma. 1968; 8(6):1049–1051. [PubMed: 5722120]

22. Wolbarst ABWAJ, Nemhauser JB, Christensen DM, Hendee WR. Medical Response to a Major Radiologic Emergency: A Primer for Medical and Public Health Practitioners. Radiology. 2010; 254(3):660–677. [PubMed: 20177084]

23. Dicarlo ALR N, Hatchett RJ. Radiation Combined Injury: Overview of NIAID Research. Health phys. 2010; 98(6):863–867. [PubMed: 20445395]

24. Fukuzuka K, Rosenberg JJ, Gaines GC, Edwards CK 3rd, Clare-Salzler M, MacKay SL, et al. Caspase-3-dependent organ apoptosis early after burn injury. Ann Surg. 1999; 229(6):851–8. discussion 8-9. [PubMed: 10363899]

25. Ramzy PIW SE, Irtun OI, Hart DW, Thompson JC, Herndon DN. Gut Epithelial Apoptosis after Severe Burn: Effects of Gut Hypoperfusion. J Am Coll Surg. 2000; 190(3):281–287. [PubMed: 10703852]

26. Rao R. Occludin phosphorylation in regulation of epithelial tight junctions. Ann N Y Acad Sci. 2009; 1165:62–68. [PubMed: 19538289]

27. Chen LW, Wang JS, Hwang B, Chen JS, Hsu CM. Reversal of the effect of albumin on gut barrier function in burn by the inhibition of inducible isoform of nitric oxide synthase. Archives of surgery. 2003; 138(11):1219–25. [PubMed: 14609870]

28. Tawa P, Hell K, Giroux A, Grimm E, Han Y, Nicholson DW, et al. Catalytic activity of caspase-3 is required for its degradation: stabilization of the active complex by synthetic inhibitors. Cell Death Dif. 2004; 11(4):439–447.

29. Vercammen D, Beyaert R, Denecker G, Goossens V, Van Loo G, Declercq W, et al. Inhibition of caspases increases the sensitivity of L929 cells to necrosis mediated by tumor necrosis factor. J Exp Med. 1998; 187(9):1477–1485. [PubMed: 9565639]

30. Kroemer G, Galluzzi L, Vandenabeele P, Abrams J, Alnemri ES, Baehrecke EH, et al. Classification of cell death: recommendations of the Nomenclature Committee on Cell Death 2009. Cell Death Dif. 2009; 16(1):3–11.

31. Imre G, Larisch S, Rajalingam K. Ripoptosome: a novel IAP-regulated cell death-signalling platform. J Mol Cell Biol. 2011; 3(6):324–326. [PubMed: 22114055]

32. Mendoza AN CJ, Charles AG, Kartchner LB, Brickey WJ, Khoury AL, Sempowski GD, Ting JP, Cairns BA, Maile R. Radiation combined with thermal injury induces immature myeloid cells. SHOCK. 2012; 38(5):532–42. [PubMed: 23042190]

33. Vanlangenakker N, Bertrand MJ, Bogaert P, Vandenabeele P, Vanden Berghe T. TNF-induced necroptosis in L929 cells is tightly regulated by multiple TNFR1 complex I and II members. Cell Death Dis. 2011; 2:e230. [PubMed: 22089168]

34. Shen L, Black ED, Witkowski ED, Lencer WI, Guerriero V, Schneeberger EE, et al. Myosin light chain phosphorylation regulates barrier function by remodeling tight junction structure. J Cell Sci. 2006; 119(Pt 10):2095–2106. [PubMed: 16638813]

35. Zahs A, Bird MD, Ramirez L, Turner JR, Choudhry MA, Kovacs EJ. Inhibition of long myosin light-chain kinase activation alleviates intestinal damage after binge ethanol exposure and burn injury. Am J Physiol Gastrointest Liver Physiol. 2012; 303(6):G705–712. [PubMed: 22790598]
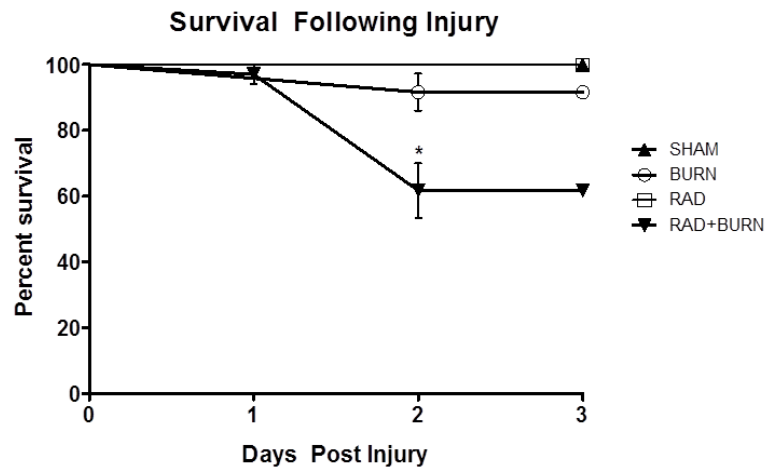
Survival Following Injury

Figure 1.
Decreased survival 72 hr post-injury in CRI. Rare death in burn injury alone is illustrated with 87.5% survival 3 days post-injury. Mortality in the CRI treated group was 41.2% (*p<0.05). Findings are consistent with those previously published by our group using this model (16). Representative of three experiments, n= 11-34 animals per injury group.
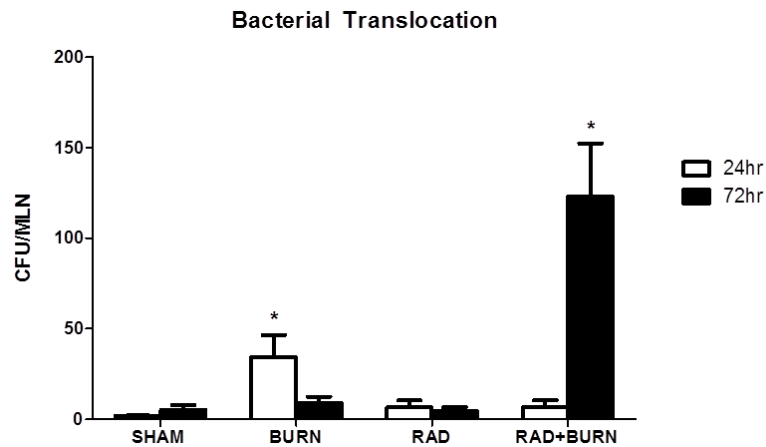
Figure 2.
Evidence of bacterial translocation following CRI. At 24 hr post injury burn alone animals exhibited a 50-fold increase in translocation relative to sham. A 100-fold increase in mesenteric lymph node bacterial translocation relative to sham was present at 72 hr following combined radiation injury, whereas burn alone is similar to sham at the same time point. Levels presented as CFU/MLN ± SEM. *p<0.05 vs. all injury groups at the same time point. Experiments at 24 hr were repeated once, n=5-6 animals per injury group. Experiments at 72 hr were repeated twice, n= 11-22 animals per injury group.
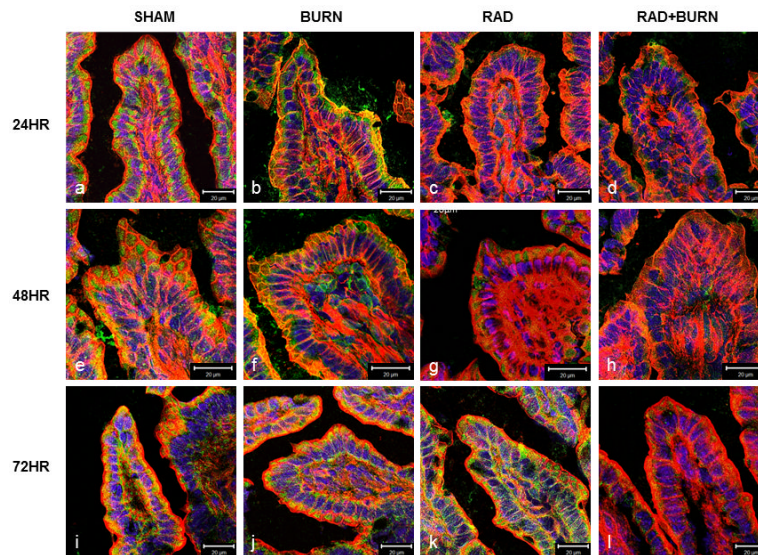
Figure 3.
CRI Disrupts tight junction protein localization. Sections of terminal ileum from sham, burn alone, radiation alone and CRI were examined by immunofluorescence at 24 (a-d), 48 (e-h) and 72 hr (i-l). Frozen ileum sections were stained with antibodies against occludin (green) as well as phalloidin (red) and nuclei (blue), examined at an original magnification of 400×, and photographed. Colocalization (yellow) occurs at interfaces between gastrointestinal epithelial cells. Decreased colocalization is evident in animals exposed to radiation, either alone or combined with burn. Most severe decreases occurred at 24 and 48 hr post injury in both groups (c, d, g, h). Radiation alone had improved staining by 72 hr post injury (k), whereas CRI remains diminished (l). Images are representative of n=4-8 animals per injury group at each time point. Scales in each image panel represent a distance of 20 μm at that specific magnification.
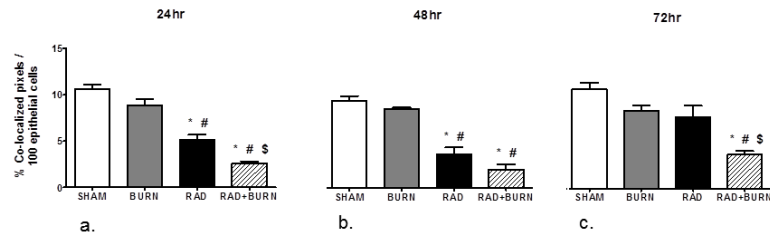
Figure 4.
Decreases in percent co-localization of occludin were most severe following CRI. Utilizing images from immunofluorescence studies, tissue sections were analyzed for co-localized pixels representative of occludin with actin staining at 24 (a), 48 (b), and 72 hr (c). Co-localization is presented as % colocalized pixels/100 epithelial cells. Sham animals averaged approximately 10% co-localization at all time points with burn alone being similar. Radiation alone and CRI treated animals had decreased quantification of colocalized pixels following injury at 24 and 48 hr (a, b). By 72 hr post injury CRI remained statistically lower than all other groups, whereas radiation alone approached sham levels (c). *p<0.05 vs. SHAM, #p<0.05 vs. BURN, $p<0.05 vs. RAD. Representative of n=4-8 animals per injury group at each time point.
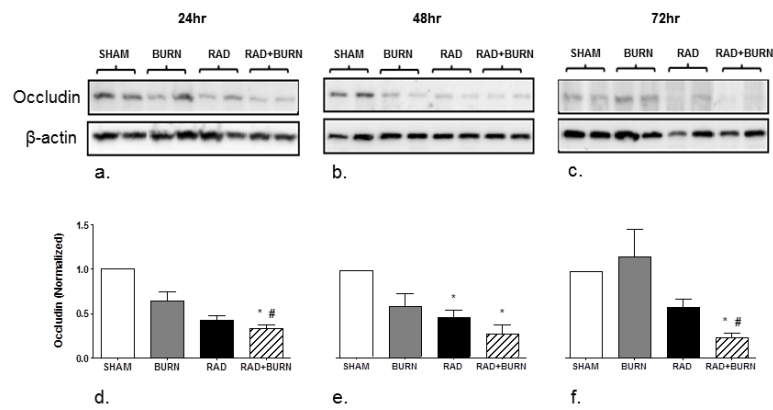
Figure 5.
Changes in occludin by western blot analysis following CRI are congruent with co-localization. Homogenate of whole ileum was analyzed for levels of occludin at 24 (a), 48 (b), and 72 hr (c) post-injury. Densitometry was performed on bands and is expressed as occludin (Normalized). Values were decreased relative to sham at 42% and 33% at 24 hr in radiation alone and CRI respectively (d). This trend persisted at 48 hr with levels that were 46% and 27% of sham (e). At 72 hr post-injury CRI remained lower relative to both sham and burn alone (24%), whereas radiation alone was no longer different (f). *p<0.05 vs. SHAM. #p<0.05 vs. BURN. Images are representative of 2 experiments, n=6-8 animals per injury group at each time point.
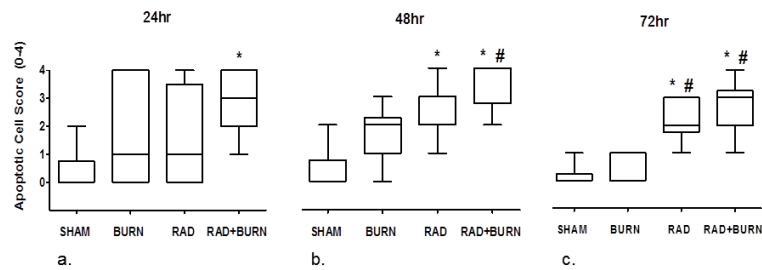
Figure 6.
Evidence of increased apoptosis at 72 hr following CRI. Quantification of apoptotic cells was performed by a pathologist in a blinded fashion at 24 (a), 48 (b) and 72 hr (c) post-injury. Sham animals had median scores of 0 apoptotic cells present at all time points. Burn injury alone had median scores of 2, 1 and 0 at 24, 48 and 72 hr respectively. Radiation alone animals had a median score of 1 and 2 at 24 hr and 48 hr respectively. Apoptosis remained elevated at 72 hr with a median score of 2. Apoptotic cells were persistently elevated following CRI, with values of 3, 4 and 3 at 24, 48 and 72 hr respectively. Data are shown as median with range. * $p < 0.05$ vs. SHAM. # $p < 0.05$ vs. BURN. Representative of three experiments per time point, n=8-14 animals per injury group.
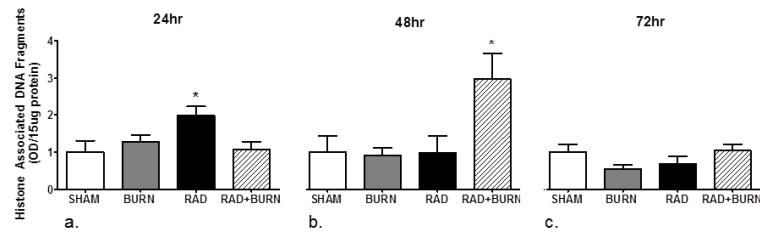
Figure 7.
Quantification of apoptosis by histone-associated DNA fragments indicates prolonged cell death at 48hr following CRI. Cell death detection utilizing ELISA for histone-associated DNA-fragments at 24 (a), 48 (b) and 72 hr (c) time points after injury. Radiation alone treated animals had a 2-fold increase in apoptosis relative to sham at 24 hr post-injury. CRI was 3 times higher than sham at 48 hr post-injury. Data are shown as mean + SEM. *p <0.05 versus SHAM, BURN, and RAD. Experiments were repeated once, n=6-10 animals per injury group at each time point.
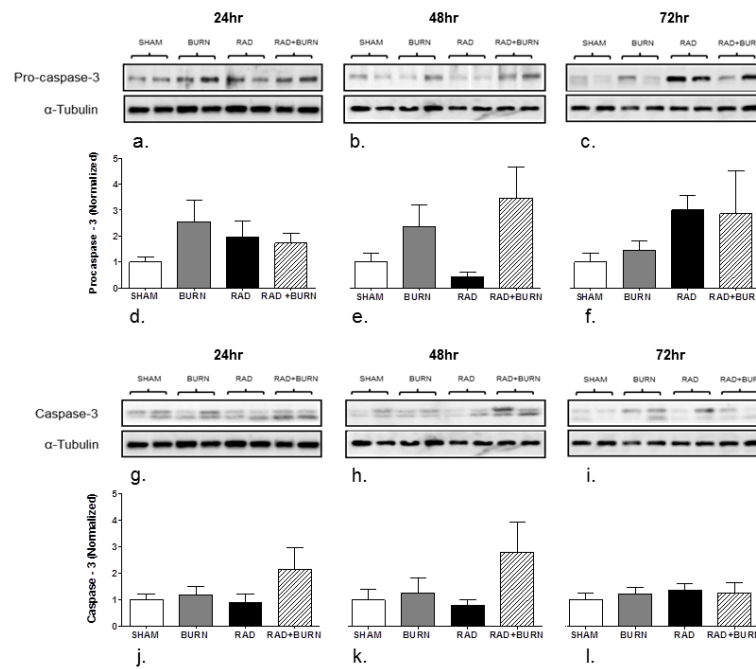
Figure 8.
Trends towards elevated pro-caspase-3 and caspase-3 by western blot analysis were not statistically significant. Homogenate of whole ileum was analyzed for levels of pro-caspase-3 (35 kDa) at 24 (a), 48 (b), and 72 hr (c). Similarly, Caspase-3 (13kDa) was measured at 24 (g), 48 (h), and 72 hr (c) post-injury. Densitometry at 24, 48, and 72 hr is expressed as procaspase-3 (Normalized) (d-f) and caspase-3 (Normalized) (j-l). Levels of procaspase-3 and caspase-3 trended towards significance at 48 hr post-injury, but did not reach significance. Images are representative of 3 experiments, n=8-14 animals per injury group at each time point.
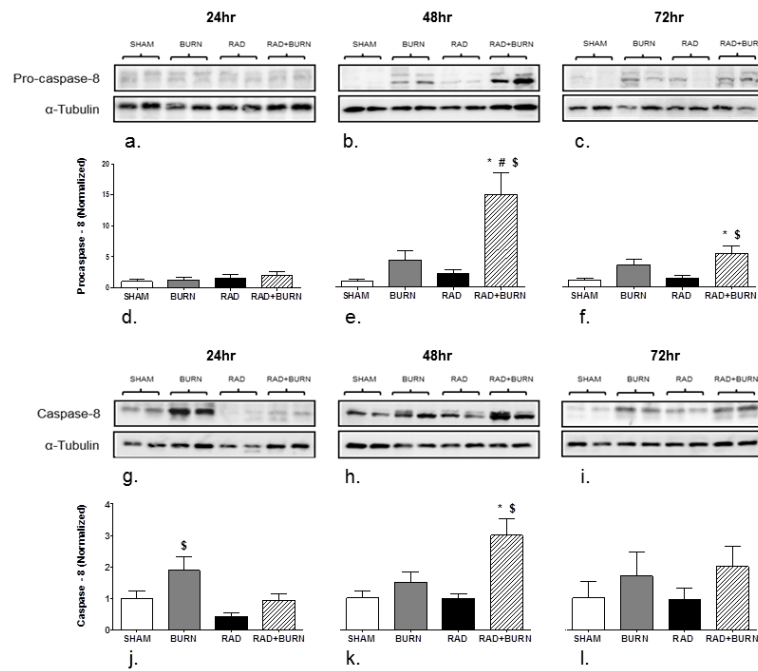
Figure 9.
Increased pro-caspase-8 and caspase-8 levels were present at 48 hr post injury in CRI.
Homogenate of whole ileum was analyzed for levels of pro-caspase-8 at 24 (a), 48 (b), and
72 hr (c). Similarly, caspase-8 was measured at 24 (g), 48 (h), and 72 hr (i) post-injury.
Densitometry at 24, 48 and 72 hr is expressed as Procaspase-8 (Normalized) (d-f) and
Caspase-8 (Normalized) (j-l). Procaspase-8 was 15 fold higher relative to sham at 48 hr and
remained elevated relative to sham and radiation alone at 72 hr. Caspase-8 levels were
double those of sham in burn alone at 24 hr and three times higher in CRI relative to sham at
48 hr post injury. All injury groups returned to sham levels by 72 hr. *p<0.05 vs. SHAM,
#p<0.05 vs. BURN, $p<0.05 vs. RAD. Images are representative of 3 experiments, n=8-12
animals per injury group at each time point.